Snow scavenging and phase partitioning of nitrated and oxygenated aromatic hydrocarbons in polluted and remote environments in central Europe and the European Arctic

Pourya Shahpoury[1,2], Zoran Kitanovski[1,3], Gerhard Lammel[1,4]

[1]Multiphase Chemistry Department, Max Planck Institute for Chemistry, Mainz, Germany

[2]Air Quality Research Division, Environment and Climate Change Canada, Toronto, Canada

[3]Department for Food Chemistry, National Institute of Chemistry, Ljubljana, Slovenia

[4]Research Centre for Toxic Compounds in the Environment, Masaryk University, Brno, Czech Republic

Correspondence to: Pourya Shahpoury (p.shahpoury@mpic.de)

Abstract

Nitrated and oxygenated polycyclic aromatic hydrocarbons (N/OPAHs) are emitted in combustion processes and formed in polluted air. Their precipitation cycling has hardly been studied. Fresh snow samples at urban and rural sites in central Europe, as well as surface snow from a remote site in Svalbard were analysed for 17 NPAHs, 9 OPAHs, and 11 nitrated mono-aromatic hydrocarbons (NMAHs), of which most N/OPAHs as well as nitrocatechols, nitrosalicylic acids, and 4-nitroguaiacol are studied for the first time in precipitation. In order to better understand the scavenging mechanisms, the particulate mass fractions (Θ) at 273K were predicted using a multiphase gas-particle partitioning model based on polyparameter linear free energy relationships. $\sum$NPAH concentrations were 1.2-17.6 and 8.8-19.1 ng L^{-1} at urban and rural sites, whereas $\sum$OPAHs were 0.3-1.1 and 0.5-2.4 µg L^{-1} at these sites, respectively. Acenaphthoquinone and 9,10-anthraquinone were predominant in snow dissolved and particulate phase, respectively. NPAHs were only found in the particulate phase with 9-nitroanthracene being predominant followed by 2-nitrofluoranthene. Among NMAHs, 4-nitrophenol showed the highest abundance in both phases. The levels found for nitrophenols were in the same range or lower than those reported in the 1980s and 1990s. The lowest levels of $\sum$OPAHs and $\sum$NMAHs were found at the remote site (9.2 and 390.5 ng L^{-1}, respectively). N/OPAHs preferentially partitioned in snow particulate phase in accordance with predicted Θ, whereas NMAHs were predominant in the dissolved phase, regardless of Θ. It is concluded that the phase distribution of non-polar N/OPAHs in snow is determined by their gas-particle partitioning prior to snow scavenging, whereas that for polar particulate phase substances, i.e. NMAHs, is determined by an interplay between gas-particle partitioning in the aerosol, particle mass size distribution, and dissolution during in- or below-cloud scavenging.

Atmospheric
Chemistry
and Physics
Discussions

Open Access

1 Introduction

Nitrated and oxygenated polycyclic aromatic hydrocarbons (N/OPAHs) are formed primarily by oxidation of parent PAHs during combustion of fossil fuels as well as biomass burning, and secondarily through reactions of PAHs with atmospheric oxidants, such as O_3, OH and NO_x (Walgraeve et al., 2010; Bandowe and Meusel, 2017). N/OPAHs were

5 found in emissions from gasoline, diesel and biodiesel (Pham et al., 2013; Zielinska et al., 2004; Karavalakis et al., 2010), biomass and coal burning (Ding et al., 2012; Shen et al., 2012; Vicente et al., 2016; Shen et al., 2013a; Shen et al., 2013b; Huang et al., 2014) and solid waste incineration (Watanabe and Noma, 2009). These substance groups were also suggested to play a role in light absorption properties of biomass burning particulate matter (PM) (Lin et al., 2016). Some NPAHs, e.g. 3-nitrofluoranthene (3-NFLT) and 1-nitropyrene (1-NPYR), are associated specifically

10 with combustion sources, whereas others such as 2-nitrofluoranthene (2-NFLT) and 2-nitropyrene (2-NPYR) are produced through gas phase reaction of FLT and PYR with OH radicals and NOx (Arey et al., 1986; Bandowe and Meusel, 2017). NPAHs are also formed through reactions in the aerosol condensed phase (Keyte et al., 2013; Jariyasopit et al., 2014). Photolysis of NPAHs results in the formation of other oxygenated and nitrated species such as hydroxynitro-PAHs, quinones, and nitrated quinones (Bandowe and Meusel, 2017). Unlike NPAHs, there is no

15 agreement on distinct formation pathways of individual OPAHs – to various extents, they originate from both primary and secondary sources (Walgraeve et al., 2010; Zhuo et al., 2017). Many N/OPAHs are suggested to be more mutagenic than their parent species and are also classified as possible carcinogens (Finlayson-Pitts and Pitts, 2000; Lammel, 2015). Moreover, quinones, a prominent sub-class of OPAHs, are precursors of environmentally persistent free radicals (Borrowman et al., 2016) and reactive oxygen species (Chung et al., 2006; Charrier et al., 2014), inducing

20 oxidative stress and inflammatory reactions in organisms, which may lead to cellular damage, respiratory and cardiovascular disease (Lodovici and Bigagli, 2011; Møller et al., 2014; Kelly and Fussell, 2017).

Nitrated mono-aromatic hydrocarbons (NMAHs) are composed of several chemically related compound classes such as: nitrophenols, nitroguaiacols, nitrocatechols and hydroxy-nitrobenzoic (i.e. nitrosalicylic) acids, which among others contain nitro, hydroxyl and carboxyl functionalities (Chow et al., 2016). Nitrophenols are emitted from primary

25 sources, particularly biomass burning but also traffic exhaust, or formed in secondary processes – nitration of precursors such as phenol in the atmosphere (Harrison et al., 2005). Nitrocatechols and nitrosalicylic acids are mainly secondary oxidation products of substituted phenols (alkylphenols, methoxyphenols, hydroxybenzoic acids) emitted in primary aerosols from biomass (e.g. wood) burning (Iinuma et al., 2007; Iinuma et al., 2010; Kitanovski et al., 2012; Kahnt et al., 2013; Chow et al., 2016). NMAHs are ecotoxic (Pflieger and Kroflič, 2017) while little is known

30 about human toxicity (Huang et al., 1995; Harrison et al., 2005; Kovacic and Somanathan, 2014). Due to nitrophenol phytotoxic potential, the research on them in precipitation was fostered during the late 1980s and early 1990s in relation with research on forest decline in central Europe (Rippen et al., 1987; Leuenberger et al., 1988; Herterich and Herrmann, 1990). Last but not least, NMAHs significantly contribute to the light absorptive properties of PM organic carbon (Mohr et al., 2013; Hinrichs et al., 2016; Bluvshtein et al., 2017; Teich et al., 2017) and can influence climate

35 by altering Earth's albedo.

Semi-volatile organic compounds (SOCs) in the atmosphere are subject to removal by dry particle deposition and wet scavenging. The latter consists of two processes – i.e. particle scavenging and gas scavenging. The particle scavenging

Atmospheric
Chemistry
and Physics
Discussions

is relevant for SOCs that show higher affinity towards particulate phase (Shahpoury et al., 2015). This is affected by SOC gas-particle partitioning (GPP) in the aerosol, a process controlled mainly by the substance molecular structure, PM chemical composition, and ambient temperature (Shahpoury et al., 2016). The magnitude of SOC sorption to PM is defined by its particulate mass fraction, Θ Eq. (1):

$$\Theta = c_p/(c_p + c_g) \tag{1}$$

5   where c_p and c_g are concentrations of SOC (ng m^{-3}) in the particulate and gas phase, respectively. The gas scavenging is relevant for substances which demonstrate minimum interaction with PM and therefore remain to various extents in the gas phase. Although gas scavenging is affected by GPP, the actual removal from the atmosphere is due to substance dissolution in cloud or rain droplets or sorption to snowflakes or other ice hydrometeors (Hoff et al., 1995; Bartels-Rausch et al., 2014). Following wet scavenging, SOC in the gas and particulate phases in the atmosphere

10   accumulate in precipitation dissolved and particulate phases, respectively. The fraction of SOC removed by particle scavenging is given by Θ_w Eq. (2):

$$\Theta_w = c_{pp}/(c_{pp} + c_{pd}) \tag{2}$$

where c_{pp} and c_{pd} are analyte concentrations (ng L^{-1}) in precipitation particulate and dissolved phases, respectively. It has been shown that the magnitude of particle scavenging is generally higher than gas scavenging for *hydrophobic* SOCs such as PAHs (Atlas and Giam, 1988; Bidleman, 1988; Shahpoury et al., 2015). In principle, for such substances

15   one could apply Θ as an indicator for predicting the SOC wet *particle* scavenging – i.e. the higher the Θ at a given temperature, the more efficient is the scavenging. However, it is not known if this concept also applies to *hydrophilic* SOCs which may also demonstrate high Θ, and whether it is GPP or another process such as dissolution in water or a combination of both that determines the substance wet scavenging pathways.

There is currently very limited information in the literature about the occurrence of N/OPAHs and NMAHs in

20   precipitation, except for small number of OPAHs (Kawamura and Kaplan, 1983) and nitrophenols: 4-nitrophenol (4-NP), several methyl-nitrophenol isomers as well as dinitrophenols (2,4-dinitrophenol (2,4-DNP) and 2-methyl-4,6-dinitrophenol (i.e. dinitro-*ortho*-cresol, DNOC) were the most frequently measured nitrophenols in precipitation in urban and rural Europe (Leuenberger et al., 1988; Alber et al., 1989; Herterich and Herrmann, 1990; Levsen et al., 1990; Levsen et al., 1991; Levsen et al., 1993; Schüssler and Nitschke, 2001; Bossi et al., 2002; Kohler and Heeb,

25   2003; Asman et al., 2005; Belloli et al., 2006; Jaber et al., 2007; Schummer et al., 2009), in North America (Ganranoo et al., 2010), and Antarctica (Vanni et al., 2001) (Table S1).

The aims of the present study were (1) to investigate the presence of N/OPAHs and NMAHs in the dissolved and particulate phases of fresh snow, (2) estimate the substance particulate mass fractions in the atmosphere using a multiphase GPP model, based on poly-parameter linear free energy relationships (ppLFER), and (3) determine the

30   substance fractions removed by wet particle scavenging, and explore the effect of GPP vs. water solubility on target compound wet scavenging.

Atmospheric
Chemistry
and Physics
Discussions

2 Experimental

2.1 Sampling

Snow samples were collected between winter 2015 and 2017 from three locations in Germany, i.e. Mainz (Ub1 and 4; urban-residential, ≈200000 inhabitants), Winterberg (Rr1) and Altenberg (Rr2; rural, >10 km from small towns),

5   two locations in Inn Valley, Austria, i.e. Götzens (Ub2; urban-residential of a mid-sized city, Innsbruck, ≈140000 inhabitants) and Kolsassberg (Rr3; rural, 10-20 km from city and towns), two locations in the Czech Republic, i.e. Ostrava (Ub3; urban, conurbation with ≈700000 inhabitants) and Pustá Polom (Rr4 and 5; rural, 20 km upwind from Ostrava), and one location in the Arctic, Tempelfjorden, Svalbard (Rm 1, remote, 50-80 km from small towns). The sample site details are shown in Table 1. Fresh snow samples (all sites, except Tempelfjorden) were collected by

10   placing several polypropylene trays (0.25 m^2 each) on the ground prior to snowfall. To this end, the snow forecast for a number of pre-selected sites was monitored on daily basis. Both collection trays and bottles were pre-cleaned prior to sample collection in the lab using detergent, tap water, deionized water, and high-purity ethanol. The snow was transferred with compaction in amber 2-L bottles and kept frozen at -18°C until analysis. Dry and light surface snow (0-5 cm deep, somewhat harder at the surface), which had fallen 3-2 days before, was collected at Tempelfjorden and

15   stored in pre-cleaned amber bottles. Following this sample collection and storage procedure, we rely on exclusion of significant phase change during storage and prior to analysis.

2.2 Sample processing

The samples were thawed at room temperature in the lab, and the meltwater was passed through a pre-assembled filtration-extraction setup (Fig. S1), allowing simultaneous separation of meltwater particulate phase and extraction

20   of dissolved phase. The setup consisted of a pre-assembled sterile analytical filter funnel (250 mL, Nalgene, Thermo Scientific, Waltham, MA, USA), connected to a solid-phase extraction disk (Bakerbond Speedisk, J.T. Baker, the Netherlands) using a Teflon adaptor designed in-house (Fig. S1). This was assembled on a J.T. Baker extraction station connected to a vacuum pump. A steady sample flow was established between the filter funnel and Speedisk throughout sample processing, by occasionally applying vacuum, where needed. The pH of meltwater samples was 4.5-5.

25   ### 2.3 N/OPAH extraction and chemical analysis

0.22 μm cellulose nitrate filter in 250 mL analytical filter funnel and octadecyl (C18) Speedisk were used for N/OPAHs extraction. Speedisks were pre-conditioned with 50 mL of methanol followed by 10 mL of deionized water, and spiked with a mixture of deuterated standards, containing 75 ng of 1-nitronaphthalene-d_7, 2-nitrofluorene-d_9, 9-nitroanthracene-d_9, 3-nitrofluoranthene-d_9, 1-nitropyrene-d_9, 6-nitrochrysene-d_{11}, 9,10-anthraquinone-d_8, and 9-

30   fluorenone-d_8. Filter papers containing particulate phase were spiked with the same standard mixture after sample processing prior to their extraction. After loading the samples, Speedisks were capped with aluminium foil and dried by pumping air through them for 5 min.

The filter papers containing the particulate phase were extracted using a previous method (Albinet et al., 2014). Briefly, each filter paper was placed in a glass centrifuge tube (Duran, Schott, Mainz, Germany) and added with 7 mL of dichloromethane (DCM). The centrifuge tubes were capped with screw caps containing PTFE lining. Each sample was vortexed for 1.5 min, passed through a glass funnel plugged with a small amount of deactivated glass wool (in

5   order to remove residual sample matrix), and concentrated to 0.5 mL using a Turbovap II (Biotage, Uppsala, Sweden). The extracts were later loaded on a pre-conditioned 500 mg SiO_2 cartridge (Macherey-Nagel, Weilmünster, Germany), and eluted with 9 mL of 65:35 *n*-hexane-DCM. The dissolved phase samples enriched on C18 Speedisks were eluted with 40 mL of 1:1 *n*-hexane-DCM. All extracts from particulate and dissolved phase were concentrated to 0.5 mL and the solvent was exchanged to ethyl acetate. The sample volumes were further adjusted to 0.3 mL and transferred to 2-

10   mL vials containing pre-baked 0.4-mL glass inserts for further analysis. All solvents used for N/OPAH analysis were Suprasolv grade (Merck, Darmstadt, Germany).

The samples were analysed using a Trace 1310 gas chromatograph (GC, Thermo Scientific, Waltham, MA, USA) coupled to a TSQ8000 Evo triple-quadrupole mass selective detector (MS/MS, Thermo Scientific) in negative chemical ionization and selected ion monitoring (SIM) modes. The analyte separation was achieved on a J&W DB-

15   5ms column (30m + 10 m integrated guard, 0.25 mm ID, 0.25 µm film thickness, Santa Clara, CA, USA) with helium (99.9999%; Westfalen AG, Münster, Germany) as carrier gas at 1 mL min^{-1} flow rate. The GC operating conditions were as follows: the GC oven was held at 60°C for 2 min, then ramped to 180°C at 15 °C min^{-1}, followed by a 5°C min^{-1} ramp to 280°C and final hold time of 15 min. The injection port temperature was set to 250°C and operated in pulsed splitless mode (30 psi pulsed pressure for 1.5 min, and splitless time of 1.8 min). MS transfer line and ion

20   source temperature were set to 290 and 230°C, respectively. Methane (>99.9995, Messer, Bad Soden, Germany) was used as ionization gas with 1.5 mL min^{-1} flow rate. Emission current and electron energy were set to 100 µA and -70 eV, respectively. The samples were analysed for N/OPAHs listed in Table 2. Each target analyte was identified using its retention time and quantification ion (Table 2). The analyte quantification was done using the internal method with 11-point calibration curves ranging from 0.25-1000 pg µL^{-1}.

25   **2.4 NMAH extraction and chemical analysis**

0.22-micron cellulose acetate filter in the 250 mL analytical filter funnel and divinylbenzene hydrophilic Speedisk were used for NMAH extraction. The detailed analytical method is described in a companion paper (Kitanovski and Naumoska, in preparation). Briefly, the pre-conditioned Speedisk was spiked with 100 ng of 4-nitrophenol-d$_4$, the sample (250 mL) was acidified with 2 mL of formic acid, and passed through the disk. The elution of NMAHs from

30   the disks was done using mixture of acetonitrile-methanol containing 3.4 µM ethylenediaminetetraacetic acid (EDTA). The presence of EDTA in the elution solvent was necessary for complete recovery of the NMAHs from the polymeric disks. The SPE extracts were further concentrated to near dryness using Turbovap II and later dissolved in 3:7 methanol-ammonium formate buffer (pH 3) containing EDTA. The PM retained on the cellulose acetate filters was spiked with the same quantity of 4-nitrophenol-d$_4$ and extracted using a previously published procedure (Kitanovski

35   et al., 2012). Briefly, the particles were extracted using methanol containing 3.4 µM EDTA with agitation in an

Atmospheric
Chemistry
and Physics
Discussions

ultrasonic bath. The final extracts were concentrated to near dryness, and dissolved in 3:7 methanol-ammonium formate buffer (pH 3) containing EDTA. All samples were analyzed using a 1200 Series liquid chromatograph (LC; Agilent Technologies, Santa Clara, CA, USA) coupled to a 6130 single-quadrupole MS (Agilent Technologies) with an electrospray ionization (ESI) source. Separation was achieved on an Atlantis T3 column (150 × 2.1 mm ID, 3 μm;

5   Waters, Milford, MA, USA), thermostated at 30°C during sample analysis. The NMAH elution was done using 30:15:55 methanol-tetrahydrofuran-aqueous ammonium formate buffer (5 mM, pH 3) mobile phase in isocratic mode. The deprotonated NMAHs [M-H]$^-$ listed in Table 2 were detected in negative ion ESI and SIM modes. The analyte quantification was done using the internal calibration method in concentration range 1-500 pg μL^{-1}.

2.5 Quality control

10   Field blanks were prepared during sample collection by exposing the pre-cleaned sample bottles with open cap to air for 5 min at the sites. The inner wall of the bottles was rinsed with 500 mL of deionized water in the lab and processed as field blank along with the rest of samples. Limits of quantification (LOQ) for analytes were calculated based on instrument detection limits (IDL), which in turn are determined using 3 times the chromatogram baseline noise level. IDL values were used in cases where analyte concentrations in blanks were <IDL. Where analyte concentrations in

15   samples exceeded the limit of quantification (LOQ: mean blank concentrations +3 standard deviations), the mean blank concentrations were subtracted from those in the corresponding samples.

2.6 Estimation of particulate mass fractions

The Θ for target analytes were estimated using modelled GPP constants, K_P (m^{3}g^{-1} at 273.15 K), which were calculated using a multiphase ppLFER model (Shahpoury et al., 2016). The model differentiates between various organic and

20   inorganic phases of PM, and accounts for absorption into water soluble organic matter (WSOM) and organic polymers (OP), as well as adsorption onto black carbon, (NH$_4$)$_2$SO$_4$ and NaCl, Eq. (3):

$$K_P \ (\mathrm{m^3_{air} \ g^{-1}_{PM}}) = [(K_{BC} \times a_{BC} \times f_{BC} + K_{(NH_4)_2SO_4} \times a_{(NH_4)_2SO_4} \times f_{(NH_4)_2SO_4} + K_{NaCl} \times a_{NaCl} \\ \times f_{NaCl}) + (K_{DMSO}/\rho_{DMSO} \times f_{WSOM} + K_{PU} \times f_{OP})] \tag{3}$$

where K_{BC}, $K_{(NH_4)_2SO_4}$, and K_{NaCl} are the target substance partitioning coefficients (mol m$^{-2}_{surface}$/mol m$^{-3}_{air}$) for black carbon/diesel soot, (NH$_4$)$_2$SO$_4$ and NaCl (the last two represent secondary inorganic aerosols), respectively, a_{BC}, $a_{(NH_4)_2SO_4}$, and a_{NaCl} are the adsorbent specific surface areas (m$^2_{surface}$ g$^{-1}_{adsorbent}$), and f_{BC}, $f_{(NH_4)_2SO_4}$, and f_{NaCl} are their

25   mass mixing ratios in PM (g$_{adsorbent}$ g$^{-1}_{PM}$). For a_{BC}, the geometric mean of 18.21 m^2 g^{-1} was calculated from the values reported for traffic, wood, coal, and diesel soot (Jonker and Koelmans, 2002), whereas, $a_{(NH_4)_2SO_4}$, and a_{NaCl} of 0.13 and 0.10 m^2 g^{-1} were taken from Goss et al., (2003). K_{DMSO} (m$^3_{air}$ m$^{-3}_{DMSO}$) and K_{PU} (m$^3_{air}$ g$^{-1}_{PU}$) are the substance partitioning (absorption) coefficients for dimethyl sulfoxide-air and polyurethane-air partitioning systems; ρ_{DMSO} is dimethyl sulfoxide density (g m^{-3}); f_{WSOM} and f_{OP}, are mass mixing ratios of absorbing phases (g$_{absorbent}$ g$^{-1}_{PM}$),

Atmospheric
Chemistry
and Physics
Discussions

corresponding to f_{OM} (the mixing ratio of total organic matter in PM) $\times 0.60$ and $f_{OM} \times 0.40$, respectively. The correction factors of 0.60 and 0.40 were estimated based on the data from Rogge et al., (1993). We assumed two scenarios for model calculations: $f_{BC} = 0.03$ and $f_{OM} = 0.30$, and $f_{BC} = 0.06$ and $f_{OM} = 0.60$. This resulted in f_{WSOM} and f_{OP} of 0.18 and 0.12, and 0.36 and 0.24 for the two scenarios, respectively. The contribution of inorganic salts to the overall

5   sorption process was neglected. The individual partitioning constants used in the multi-phase model are calculated using substance-specific Abraham descriptors listed in Table S2 and ppLFER models listed in Table S3 (Abraham et al., 2010; Kamprad and Goss, 2007; Roth et al., 2005; Goss et al., 2003). See Shahpoury et al., (2016) for more details about calculation with multiphase model and Endo and Goss (2014) for background about ppLFER concept. The predicted K_P values were converted to Θ under two scenarios with c_{PM} of 25 and 50 µg m^{-3}, Eq. (4):

$$\theta = \frac{K_P\ c_{PM}}{(1 + K_P\ c_{PM})} \tag{4}$$

10   One must note that the ppLFER model used here predicts K_P of a substance in neutral form. In particulate phase, depending on pH of the PM aqueous phase and pK_a of the target substance, NMAHs may partly or completely deprotonate, resulting in enhanced solubility of the substance in the aqueous phase (Ahrens et al., 2012). Given the pH of samples in our study (i.e. 4.5-5), we expect 5-nitrosalicylic acid (5-NSA; see Table 2 for compound abbreviations), pK_a: 1.95 at 298 K (Aydin et al., 1997) and 3-nitrosalicylic acid (3-NSA; we expect similar pK_a as that

15   of 5-NSA) to be completely deprotonated in PM aqueous phase, whereas 2,4-DNP and DNOC, pK_a: 4.07 at 298 K (Lide, 2010) and 4.48 at 293 K (WHO, 2000), respectively, will be partly dissociated. This implies that the actual partitioning could be under-predicted. The rest of NMAHs would be present in protonated form in our study (pK_a: 4-NP: 7.15, 2-methyl-4-nitrophenol (2-M-4-NP): 7.33, 3-methyl-4-nitrophenol (3-M-4-NP): 7.33, 4-nitrocatechol (4-NC): 6.93 at 298 K; we expect pK_a values for 4-methyl-5-nitrocatechol (4-M-5-NC) and 3-methyl-5-nitrocatechol (3-

20   M-5-NC) to be close to that for 4-NC).

2.7 Air mass history analysis

The HYSPLIT (Draxler and Rolph, 2003) model was used to identify air mass histories related to the snowfall events over 3 days. The meteorological data (1°x1° resolution) used were from the Global Data Assimilation System (GDAS, NCEP, USA). Air mass changes were identified based on weather charts (Berliner Wetterkarte, 2015), except for

25   sample site in Svalbard, Rm1, as the snow fell 2-3 days prior to sample collection.

3 Results and discussion

3.1 Air mass backward trajectory analysis

For all central European sites, the air masses corresponding to the snow samples had been advected mostly from westerly directions (see air mass trajectories in Fig. S2), passing over polluted areas of central and western Europe

30   (such as in NE France/SW Germany, W and SE Germany for samples Ub1, Ub3, Rr1 and Rr2) until the last 100-200 km before precipitation started, when they had been transported over rural areas. The snowfalls leading to samples

Ub1, Ub3, Rr1, and Rr5 followed immediately frontal passages with advection from westerly directions (Fig. S2), unlike in the other precipitation events.

3.2 N/OPAH concentrations and distribution in snow

Snow dissolved and particulate phases were analysed for N/OPAHs following the method described in Sect. 2.3.
5   Among these compounds, NPAHs were only found in the snow particulate phase. On the contrary, OPAHs, 9-fluorenone (9-OFLN), acenaphthoquinone (O_2ACE), and 9,10-anthraquinone (9,10-O_2ANT) were found in nearly all dissolved phase samples, except at the remote site where 9,10-O_2ANT was not found (Fig. 1A). O_2ACE demonstrated the largest concentration range (4.1 to 779.8 ng L^{-1}) followed by 9,10-O_2ANT (< LOQ in Rm 1 sample to 89.7 ng L^{-1}), and 9-OFLN (2.6 to 45.3 ng L^{-1}). 1,2-benzanthraquinone (1,2-O_2BAA) was not found in samples Ub1 and Rm1,
10   while concentrations ranged from 0.2 to 1.3 ng L^{-1} for the rest of the samples (Fig. 1A). 1,4-naphthoquinone (1,4-O_2NAP), benzanthrone (OBAT), and benz(*a*)fluorenone (BaOFLN) were found less frequently with concentrations up to 7.1, 1.4, and 0.2 ng L^{-1}, respectively. Overall, the lowest OPAH concentrations were from the remote site, (∑ OPAHs 7.3 ng L^{-1}), while sample Ub4 was the most polluted (∑ OPAHs 834 ng L^{-1}), mainly due to the contribution of O_2ACE, followed by Rr1 (303.6 ng L^{-1}), and Rr3 (279.3 ng L^{-1}).

15   9-OFLN, 9,10-O_2ANT, 1,4-O_2NAP, and 1,2-O_2BAA were previously found in diesel exhaust (Choudhury, 1982; Cho et al., 2004) and biomass and coal burning emission (Shen et al., 2013a; Huang et al., 2014; Vicente et al., 2016, along with O_2ACE), whereas in ambient PM, 9-OFLN 9,10-O_2ANT, and 1,2-O_2BAA were attributed to both primary and secondary sources (Kojima et al., 2010; Souza et al., 2014; Lin et al., 2015; Zhuo et al., 2017). The contribution of primary sources is expected to be higher during the cold season with heating activities dominating the vehicular
20   emission (Lin et al., 2015). OBAT does not have a stable parent PAH precursor with the same number of rings in the atmosphere (Kojima et al., 2010) and, along with BaOFLN and benz(*b*)fluorenone (BbOFLN), was associated with primary combustion sources (Albinet et al., 2007; Karavalakis et al., 2010; Shen et al., 2013b; Souza et al., 2014; Huang et al., 2014; Tomaz et al., 2016; Vicente et al., 2016).

In the particulate phase of snow, four NPAHs and seven OPAHs were detected (Fig. 1B). In Rm1 only three OPAHs,
25   O_2ACE (1.7 ng L^{-1}), BaOFLN (0.15 ng L^{-1}), and 1,2-O_2BAA (0.13 ng L^{-1}), were found with relatively low concentrations. Among all detected analytes, 9,10-O_2ANT (found in Ub2, Rr1-3) showed the highest concentrations ranging from 155.6 to 242.2 ng L^{-1} followed by 9-OFLN (found in all but Rm 1, 4.0-30.3 ng L^{-1}), BaOFLN (0.15-27.3 ng L^{-1}), and 1,2-O_2BAA (0.13-23.3 ng L^{-1}). The detected NPAHs, 9-nitroanthracene (9-NANT), 2-nitrofluoranthene (2-NFLT), 1-nitronaphthalene (1-NNAP), and 2-nitronaphthalene (2-NNAP) showed relatively low
30   concentrations ranging from <LOQ-13.6 ng L^{-1} (9-NANT), <LOQ-2.6 ng L^{-1} (2-NFLT), <LOQ-1.3 ng L^{-1} (1-NNAP), and <LOQ - 0.32 ng L^{-1} (2-NNAP), respectively. NPAHs found in the present study are the most frequently detected congeners in the gas (1- and 2-NNAP) and particulate (2-NFLT and 9-NANT) phases (Dimashki et al., 2000; Bamford and Baker, 2003; Albinet et al., 2006; Tomaz et al., 2016; Bandowe and Meusel, 2017), with 2-NFLT being exclusively formed through reaction of FLT with oxidants in the atmosphere (Bandowe and Meusel, 2017) and the
35   other three NPAHs being produced by both primary and secondary sources (Zhuo et al., 2017). One must also note

the possibility of NPAH conversion to OPAHs in the atmosphere. For instance, formation of 1,4-O_2NAP and 9,10-O_2ANT following photolysis of 1-NNAP and 9-NANT was suggested by previous studies (Keyte et al., 2013; Bandowe and Meusel, 2017); this might have contributed to the observed concentration patterns in the present study. Overall, the lowest and highest $\sum$ N/OPAH concentrations in the particulate phase were found at Rm1 (1.9 ng L^{-1}) and

5   Rr3 (359.8 ng L^{-1}), with NPAHs contributing up to 10% to the total concentrations across the samples.

Snow samples Ub3 and Rr4-5 were not phase separated for N/OPAH analysis. Of all targeted NPAHs at these sites, only 2-NFLT (11.6-19.1 ng l^{-1}) was found in the samples (Fig. 1C). Among OPAHs, OBAT, 9,10-O_2ANT, and O_2ACE showed the highest concentrations ranging from 478.3 - 758.1, 234.9 - 607.7, and 141.8 - 609.9 ng L^{-1}, respectively, whereas 1,2-O_2BAA, BbOFLN, BaOFLN, 9-OFLN, and 1,4-O_2NAP demonstrated relatively lower levels, up to 136.5,

10   106.5, 95.9, 57.6, and 18.6 ng L^{-1}, respectively (Fig. 1C). OPAH concentrations were overall higher in Rr4-5 samples than Ub3. The predominance of OBAT, 9,10-O_2ANT, O_2ACE, and 9-OFLN is consistent with findings of the previous studies for ambient PM and primary emission samples. High abundance of OBAT is of particular concern because this compound is precursor of the mutagenic 2- and 3-nitrobenzanthrone (Enya et al., 1997; Phousongphouang and Arey, 2003).

15   **3.3 NMAH concentrations and distribution in snow**

NMAHs targeted for analysis were found in all dissolved phase samples, with the exception of 4-nitroguaiacol (4-NG; Fig. 2A-B). 4-NP showed the highest concentrations ranging from 9.5 to 2155.4 ng L^{-1}, followed by 4-NC (18.2- 763.6 ng L^{-1}), 3-M-4-NP (4.6 - 547.3 ng L^{-1}), 2-M-4-NP (18.4 - 341.1 ng L^{-1}), and 5-NSA (6.6 - 313.5 ng L^{-1}). In this phase, 4-NG was exclusively found in samples from urban (Ub3 and Ub4, 155.2 and 284.7 ng L^{-1}, respectively; Fig. 2B),

20   rural (Rr4 and Rr5, 169.4 and 282.3 ng L^{-1}, respectively; Fig. 2A) and remote (Rm1, 14.8 ng L^{-1}; Fig. 2A) environments. Overall, the dissolved phase samples from Rm1 and Ub3 were the least polluted ($\sum$ NMAHs: 387.0 and 746.7 ng L^{-1}) while Ub2, Rr1, and Rr4-5 showed the highest concentrations of target compounds (1231 - 1345 ng L^{-1}) across the samples (Fig. 2A-B).

The NMAHs were found more sporadically in the snow particulate phase. 4-NP was found in all samples, with

25   concentrations ranging from 2.2 (Rr3) to 106.9 (Ub4) ng L^{-1} (Fig. 2C-D). In fact, 4-NP was the only NMAH found at the remote site Rm1 (3.5 ng L^{-1}; Fig. 2C). 4-NG was only found in Rr2 (18.5 ng L^{-1}; Fig. 2C) and Ub4 (40.8 ng L^{-1}; Fig. 2D) samples. 3- and 5-NSA were found in Ub4 particulate phase (2.9 and 13.5 ng L^{-1}, respectively; Fig. 2D), while 4- and 3-M-5-NC were found in Ub4 (5.8 and 11.4 ng L^{-1}, respectively; Fig. 2D), Rr2 (4-M-5-NC: 0.8 ng L^{-1}; Fig. 2C) and Rr5 (3-M-5-NC: 1 ng L^{-1}; Fig. 2C). In addition, 2,4-DNP and 4-NC were only found in Ub4 (2.7 and

30   36.9 ng L^{-1}, respectively; Fig. 2D), Ub3 and Rr4 (up to 2.9 ng L^{-1} for 2,4-DNP) and Rr1-2 (up to 1.3 ng L^{-1} for 4-NC). The highest concentrations of DNOC and 3-M-4-NP in the particulate phase were from the Czech sites (up to 11.8 ng L^{-1} for DNOC and 21.8 ng L^{-1} for 3-M-4-NP), with DNOC concentration being ~ 2 times higher at the urban Ub3 than at the rural and upwind site Rr4 (Fig. 2C-D). The highest particulate concentrations for 2-M-4-NP were found in Ub4 sample (39.2 ng L^{-1}; Fig. 2D). These analytes (DNOC, 2-M- and 3-M-4-NP) together with 4-NP were the most

35   abundant compounds in the particulate phase. Overall, in terms of the levels of target NMAHs in the particulate phase,

the remote site (Rm1) was the cleanest ($\sum$ NMAHs 3.5 ng L^{-1}) and the Czech sites, with the urban exceeding the rural (52.5 and 33.5 ng L^{-1} in Ub3 and Rr5, respectively) were the most polluted sites in our study.

The nitrophenol concentrations measured are in the same range with those previously reported for snow samples collected in central Europe and Antarctica (Alber et al., 1989; Vanni et al., 2001; Table S1), but usually lower (up to

5   two orders of magnitude lower) than those reported in rainwater from central and northern Europe (Leuenberger et al., 1988; Herterich and Herrmann, 1990; Levsen et al., 1991; Bossi et al., 2002; Asman et al., 2005; Schummer et al., 2009; Table S1) and the USA (Ganranoo et al., 2010; Table S1). One must note that here we report the NMAH concentrations in both particulate and dissolved phases, which was not done in the previous studies (Table S1). The dissolved phase concentrations of 4-NG in samples from urban and rural environments were comparable (~ 155-285

10 ng L^{-1}; Fig. 2A-B), indicating polluted and aged air masses with biomass burning origin (Kitanovski et al., 2014; Kroflič et al., 2015; Yang et al., 2016). These values are one order of magnitude higher than the measured concentration for the Arctic sample Rm1 (Fig. 2A). In urban samples with the exception of Ub3, nitrocatechols (4-NC and isomeric methyl-nitrocatechols) were the second most abundant NMAH species, following nitrophenols (Table S4A). This is in agreement with our current unpublished data and previous studies on winter PM samples

15 (Kitanovski et al., 2012). In contrast, in rural samples Rr3-4 and the remote sample Rm1, nitrosalicylic acids are the second most abundant NMAH species (Table S4A), which might indicate either higher stability or higher formation of these compounds during the transport of polluted air to the rural environments and the Arctic. Increased production of nitrocatechols in the urban environment due to anthropogenic activities, such as wood burning in winter, was suggested by previous studies (Kitanovski et al., 2012; Chow et al., 2016). Hydroxybenzoic acids, which are

20 precursors of nitrosalicylic acids, are primarily emitted during wood burning (Iinuma et al., 2007). Kitanovski et al., (2012) reported a high correlation between concentrations of nitrocatechols and nitrosalicylic acids (R^2 >0.8) in urban PM. This suggests secondary formation of nitrosalicylic acids as well as biomass burning as the major emission source, similar to the previous reports on nitrocatechols (Iinuma et al., 2010; Kitanovski et al., 2012; Kahnt et al., 2013; Chow et al., 2016; Caumo et al., 2016).

25 **3.4 Modelled particulate mass fractions and actual fractions removed by particle scavenging**

The target compound Θ was estimated following the method explained in Sect. 2.6. We examined three scenarios i.e., a lower, middle and upper scenario with regard to pollution: (1) with f_{BC} and f_{OM} of 0.03 and 0.30 and c_{PM} of 25 µg m^{-3}, (2) f_{BC} and f_{OM} of 0.06 and 0.60 and c_{PM} of 25 µg m^{-3}, and (3) f_{BC} and f_{OM} of 0.06 and 0.60 and c_{PM} of 50 µg m^{-3}. In fact, the 24-h mean c_{PM} for Mainz (Ub4) and the Ostrava (Ub3) sampling events was 25 and 27 µg m^{-3}, respectively.

30 No data are available from the other sites. As can be seen from Fig. 3A-C, Θ at 273 K is ~ 1 (complete sorption to PM) for 70% of the target compounds, independent of the above scenarios. The calculations showed that <20% of 1-NNAP, 2-NNAP, 1,4-O$_2$NAP, 9-OFLN, 2,4-DNP, and DNOC, and between 20 and 80% of 5-NACE, 2-NFLN, O$_2$ACE, 3-NSA, and 4-NG can be expected to be in the particulate phase at 273 K (Fig. 3). For these substances, Θ increases by up to two fold when increasing f_{BC}, f_{OM}, or c_{PM}. An interesting trend was seen for 2,4-DNP and 4-NP: the

35 presence of two nitro groups on 2,4-DNP is expected to promote stronger interactions with PM due to increased e-

donor ability, compared to 4-NP (one nitro group). However, our model calculations suggest the opposite pattern, i.e. complete sorption of 4-NP to PM, but <5% sorption for 2,4-DNP. This is largely related to intramolecular H-bonding between the H-atom of the hydroxy group and the O-atom of the nitro group in ortho position. This reduces the H-bonding ability of 2,4-DNP compared to 4-NP.

5   For substances which indicate complete sorption to PM, particle scavenging is expected to be the dominant source of wet deposition, whereas, for the rest of substances, which distribute between gas and particulate phases, both gas and particle scavenging are relevant. Accordingly, one would expect to find the substances with complete sorption to PM in precipitation particulate phase. Our observations depicted in Fig. 4A show that N/OPAHs in the present study were mainly associated with precipitation particulate phase. The exceptions were O_2ACE (70-100%), 9-OFLN (30-100%),

10   and 9,10-O_2ANT (10-100%) which were found to various extents in the dissolved phase. This trend is consistent with predicted values of Θ, particularly for O_2ACE and 9-OFLN, and to a lesser extent 9,10-O_2ANT (Fig. 3B), and supports the implied assumption that phase partitioning in air is preserved in snow.

For one of the events, Ub3, the analyte concentrations in the gas and particulate phases of the air have been determined (24h sample collected until shortly after snowfall started; Table S4B) in addition to concentrations in precipitation.

15   The total scavenging ratios (W_T; unitless) calculated for the target N/OPAHs were 10^3-10^4 (Table S4B), which fall within the range suggested for removal of polyaromatic compounds through particle scavenging (Shahpoury et al., 2015). With the exception of 1,4-O_2NAP and 9-OFLN, the calculated ratios are consistent with modelled Θ of 0.81-1 (at 273 K) for the target N/OPAHs (Table S4B) in that particle scavenging was the dominant removal mechanism.

The observation for NMAHs, however, are considerably different (Fig. 4B). These substances were mainly found in

20   the dissolved phase, including the seven analytes for which complete sorption to PM was predicted under various scenarios. Among all, 4-NP showed the highest fraction in the precipitation particulate phase and, as predicted, higher than 2,4-DNP, followed by 2-M-4-NP. The observed opposite pattern may suggest that besides GPP another process influenced the wet scavenging of NMAHs and consequently their distribution in precipitation phases. We hypothesize that following both in- and below-cloud scavenging into sub-cooled droplets, particulate-phase NMAHs would

25   dissolve into the bulk water or water layer surrounding ice hydrometeors (Hoff et al., 1995). This process is affected by the substance water solubility and, therefore, is anticipated to be most efficient for highly water soluble substances. In fact, among N/OPAHs found in the present study, the only substance that showed high enrichment in the dissolved phase was O_2ACE (Fig. 4A) with log octanol-water partitioning coefficient (log K_{OW}; unitless) of 1.95 compared to log K_{OW} of 3.03-4.98 for the other detected N/OPAHs; Fig. S3). NMAHs are highly water soluble (s = 0.3-10 g L^{-1},

30   log K_{OW} = 0.64-2.54; Fig. S3) and, therefore, are expected to undergo the abovementioned process. This hypothesis is consistent with the results of a previous study where positive correlation was found between in-cloud scavenging efficiencies of PM-bound polar organics and the substance polarity and water solubility (Limbeck and Puxbaum, 2000). This process (which potentially results in predominance of NMAHs in the dissolved phase), however, must be distinguished from the gas scavenging which was proposed by Leuenberger et al., (1985) as a dominant process for

35   removal of volatile methylated phenols, where the predominance of these substances in the dissolved phase corresponded to their abundance in the gas phase.

Atmospheric
Chemistry
and Physics
Discussions

In sample Ub3 which corresponds to known analyte concentrations in air particulate phase, W_T was found to be in the range 10^3-10^5 (Table S4B), which is relevant for wet *particle* scavenging of aromatic compounds (Shahpoury et al., 2015), and suggests that the removal of NMAHs followed a similar mechanism. Interestingly, the difference in W_T between 3- and 5-NSA (~1.4 times higher for 5-NSA) closely resembled that of estimated Θ (~1.6 times higher for 5-NSA at 273 K) for these compounds (Table S4B). However, we found noticeable differences in W_T between the NMAH subgroups, namely W_T values were higher for nitrophenols (1.3×10^4– 1.6×10^5) and nitrosalicylic acids (5.7×10^4 – 8.2×10^4) than nitrocatechols (1.1×10^3 – 2.8×10^3; Table S4B). This pattern cannot be explained by the substance GPP (compare Θ in Fig. 3C), or the order of their water solubility. Accordingly, nitrosalicylic acids are the most water soluble substances among the three subgroups, regardless of their predicted K_{OW} values shown in Fig. S3 (due to their pKa of < 2, these compounds would be completely deprotonated in our samples (pH 4-5), which enhances their water solubility. This is also reflected in them showing the lowest retention times in Table 2). Moreover, nitrocatechols are more water soluble (log K_{OW} 0.64-1.27; Fig. S3) than nitrophenols (log K_{OW} 1.68-2.43) – it must be noted that nitrocatechols and nitrophenols have pKa of > 6, which means they would be present in protonated (neutral) form in our samples. Given the above explanation, we believe that the observed differences in W_T of the subgroups were in fact related to the mass size distribution of NMAHs in the atmosphere prior to snow scavenging. According to our unpublished data from Ub3, nitrophenols were mainly associated with coarse PM fraction (~60%), followed by nitrosalicylic acids (~35%). Nitrocatechols on the other hand were exclusively associated with the fine fraction (PM$_1$; ~80%), similar to observations reported by Li et al., (2016). This mass size distribution could potentially enhance snow scavenging of nitrophenols following the *interception* of coarse particles by snowflakes – this mechanism was suggested to be important for PM in the size range of 1 μm to a few microns (Zhang et al., 2013), and its contribution is expected to increase with the particle size. It was further suggested that a combination of Brownian diffusion, interception, and inertial impaction leads to a low *snow particle-aerosol particle collection efficiency* (suggested to be the most important source of uncertainty in snow scavenging of PM) in the particle size range of 0.01-1.0 μm (Zhang et al., 2013), which could further explain the relatively low W_T values found for nitrocatechols in the present study. We conclude that an interplay between GPP and PM mass size distribution determined the mechanism and magnitude of NMAH wet scavenging, whereas water solubility contributed to their phase partitioning in snow.

Final remarks

The phase-separated concentrations of nitrated and oxygenated aromatic compounds were measured in snow from several locations in central Europe and European Arctic. For the first time, we have reported the snow concentrations for several classes of nitrated and oxygenated aromatics, such as nitrocatechols, nitrosalicylic acids, nitrated and oxygenated PAHs, and 4-nitroguaiacol. Our results showed that a model-predicted particulate mass fraction, Θ, can be reliably applied in order to predict the scavenging mechanism (gas or particle scavenging) and efficiency of *hydrophobic* N/OPAHs and, hence, their distribution in precipitation phases i.e., dissolved and particulate. This suggests that the atmospheric lifetime of N/OPAHs in relation to removal processes follows the same pattern as that of parent PAHs (Sharma and McBean, 2002). On the contrary, Θ is not a good measure for predicting the wet removal

mechanism and distribution of *hydrophilic* NMAHs in precipitation. Our data suggests that the phase distribution of polar particulate phase substances, such as NMAHs in snow is determined by an interplay between GPP in the aerosol, mass size distribution in the atmosphere, and dissolution in cloud or rain droplets, or the liquid water phase on the surface of ice hydrometeors during in- or below-cloud scavenging. This behaviour is in line with what was previously

5 shown for the effect of aerosol mass size distribution on snow scavenging (Zhang et al., 2013), and what was found for in-cloud scavenging of other polar mono- and difunctional organics, such as aliphatic alcohols, and aliphatic and monoaromatic aldehydes and carboxylic acids (Limbeck and Puxbaum, 2000), namely the polarity of these substances is a significant parameter for their scavenging when solubility is > 1 g L^{-1}. The experimental data on GPP of NMAHs is scarce in the literature, which was also not addressed here. The contribution of gaseous polar NMAHs to the total

10 scavenging, beyond the scope of this study, should be addressed, similar to other polar aliphatic and aromatic organics (Limbeck and Puxbaum, 2000).

Data availability

The dataset used in this manuscript is included in the Supplement, and further information is available from the corresponding author (p.shahpoury@mpic.de).

Competing interests

The authors declare that they have no conflict of interest.

Acknowledgements

References

Abraham, M. H., Smith, R. E., Luchtefeld, R., Boorem, A. J., Lou, R. and Acree, W. E.: Prediction of solubility of

25 drugs and other compounds in organic solvents, J. Pharm. Sci., 99, 1500–1515, doi:10.1002/jps.21922, 2010.

Ahrens, L., Harner, T., Shoeib, M., Lane, D. A. and Murphy, J. G.: Improved characterization of gas–particle partitioning for per- and polyfluoroalkyl substances in the atmosphere using annular diffusion denuder samplers, Environ. Sci. Technol., 46, 7199–7206, doi:10.1021/es300898s, 2012.

Alber, M., Böhm, H. B., Brodesser, J., Feltes, J., Levsen, K. and Schöler, H. F.: Determination of nitrophenols in rain

30 and snow, Fresenius' Zeitschrift für Anal. Chemie, 334, 540–545, doi:10.1007/BF00483573, 1989.

Atmospheric
Chemistry
and Physics
Discussions

Albinet, A., Leoz-Garziandia, E., Budzinski, H. and Villenave, E.: Simultaneous analysis of oxygenated and nitrated polycyclic aromatic hydrocarbons on standard reference material 1649a (urban dust) and on natural ambient air samples by gas chromatography–mass spectrometry with negative ion chemical ionisation, J. Chromatogr. A, 1121, 106–113, doi:10.1016/j.chroma.2006.04.043, 2006.

5 Albinet, A., Leoz-Garziandia, E., Budzinski, H. and Villenave, E.: Polycyclic aromatic hydrocarbons (PAHs), nitrated PAHs and oxygenated PAHs in ambient air of the Marseilles area (South of France): concentrations and sources, Sci. Total Environ., 384, 280–292, doi:10.1016/j.scitotenv.2007.04.028, 2007.

Albinet, A., Nalin, F., Tomaz, S., Beaumont, J. and Lestremau, F.: A simple QuEChERS-like extraction approach for molecular chemical characterization of organic aerosols: application to nitrated and oxygenated PAH derivatives (NPAH and OPAH) quantified by GC–NICIMS, Anal. Bioanal. Chem., 406, 3131–3148, doi:10.1007/s00216-014-10 7760-5, 2014.

Arey, J., Zielinska, B., Atkinson, R., Winer, A. M., Ramdahl, T. and Pitts, J. N.: The formation of nitro-PAH from the gas-phase reactions of fluoranthene and pyrene with the OH radical in the presence of NOx, Atmos. Environ., 20, 2339–2345, doi:10.1016/0004-6981(86)90064-8, 1986.

15 Asman, W. A. H., Jørgensen, A., Bossi, R., Vejrup, K. V., Bügel Mogensen, B. and Glasius, M.: Wet deposition of pesticides and nitrophenols at two sites in Denmark: measurements and contributions from regional sources, Chemosphere, 59, 1023–1031, doi:10.1016/j.chemosphere.2004.11.048, 2005.

Atlas, E. and Giam, C. S.: Ambient concentration and precipitation scavenging of atmospheric organic pollutants, Water Air Soil Pollut., 38, 19–36, doi:10.1007/BF00279583, 1988.

20 Aydin, R., Özer, U. and Türkel, N.: Potentiometric and spectroscopic determinaton of acid dissociation constants of some phenols and salicylic acids, Turkish J. Chem., 21, 428–436, 1997.

Bamford, H. A. and Baker, J. E.: Nitro-polycyclic aromatic hydrocarbon concentrations and sources in urban and suburban atmospheres of the mid-Atlantic region, Atmos. Environ., 37, 2077–2091, doi:10.1016/S1352-2310(03)00102-X, 2003.

25 Bandowe, B. A. M. and Meusel, H.: Nitrated polycyclic aromatic hydrocarbons (nitro-PAHs) in the environment – a review, Sci. Total Environ., 581–582, 237–257, doi:10.1016/j.scitotenv.2016.12.115, 2017.

Bartels-Rausch, T., Jacobi, H.-W., Kahan, T. F., Thomas, J. L., Thomson, E. S., Abbatt, J. P. D., Ammann, M., Blackford, J. R., Bluhm, H., Boxe, C., Domine, F., Frey, M. M., Gladich, I., Guzmán, M. I., Heger, D., Huthwelker, T., Klán, P., Kuhs, W. F., Kuo, M. H., Maus, S., Moussa, S. G., McNeill, V. F., Newberg, J. T., Pettersson, J. B. C., 30 Roeselová, M. and Sodeau, J. R.: A review of air–ice chemical and physical interactions (AICI): liquids, quasi-liquids, and solids in snow, Atmos. Chem. Phys., 14, 1587–1633, doi:10.5194/acp-14-1587-2014, 2014.

Belloli, R., Bolzacchini, E., Clerici, L., Rindone, B., Sesana, G. and Librando, V.: Nitrophenols in air and rainwater, Environ. Eng. Sci., 23, 405–415, doi:10.1089/ees.2006.23.405, 2006.

Berliner Wetterkarte: Daily Charts, CDROM edition, Verein Berliner Wetterkarte, e.V. Available from: 35 http://www.berliner-wetterkarte.de, 2015.

Bidleman, T. F.: Atmospheric processes, Environ. Sci. Technol., 22, 361–367, doi:10.1021/es00169a002, 1988.

Bluvshtein, N., Lin, P., Flores, J. M., Segev, L., Mazar, Y., Tas, E., Snider, G., Weagle, C., Brown, S. S., Laskin, A. and Rudich, Y.: Broadband optical properties of biomass-burning aerosol and identification of brown carbon chromophores, J. Geophys. Res. Atmos., 122, 5441–5456, doi:10.1002/2016JD026230, 2017.

40 Borrowman, C. K., Zhou, S. M., Burrow, T. E. and Abbatt, J. P. D.: Formation of environmentally persistent free radicals from the heterogeneous reaction of ozone and polycyclic aromatic compounds, Phys. Chem. Chem. Phys., 18, 205–212, doi:10.1039/c5cp05606c, 2016.

Bossi, R., Vejrup, K., Mogensen, B. and Asman, W. A.: Analysis of polar pesticides in rainwater in Denmark by liquid chromatography–tandem mass spectrometry, J. Chromatogr. A, 957, 27–36, doi:10.1016/S0021-9673(02)00312-6, 45 2002.

Atmospheric
Chemistry
and Physics
Discussions

Caumo, S. E. S., Claeys, M., Maenhaut, W., Vermeylen, R., Behrouzi, S., Safi Shalamzari, M. and Vasconcellos, P. C.: Physicochemical characterization of winter PM10 aerosol impacted by sugarcane burning from São Paulo city, Brazil, Atmos. Environ., 145, 272–279, doi:10.1016/j.atmosenv.2016.09.046, 2016.

5 Charrier, J. G., McFall, A. S., Richards-Henderson, N. K. and Anastasio, C.: Hydrogen peroxide formation in a surrogate lung fluid by transition metals and quinones present in particulate matter, Environ. Sci. Technol., 48, 7010–7017, doi:10.1021/es501011w, 2014.

Cho, A. K., Di Stefano, E., You, Y., Rodriguez, C. E., Schmitz, D. A., Kumagai, Y., Miguel, A. H., Eiguren-Fernandez, A., Kobayashi, T., Avol, E. and Froines, J. R.: Determination of four quinones in diesel exhaust particles, SRM 1649a, and atmospheric PM2.5, Aerosol Sci. Technol., 38, 68–81, doi:10.1080/02786820390229471, 2004.

10 Choudhury, D. R.: Characterization of polycyclic ketones and quinones in diesel emission particulates by gas chromatography/mass spectrometry, Environ. Sci. Technol., 16, 102–106, doi:10.1021/es00096a009, 1982.

Chow, K. S., Huang, X. H. H. and Yu, J. Z.: Quantification of nitroaromatic compounds in atmospheric fine particulate matter in Hong Kong over 3 years: field measurement evidence for secondary formation derived from biomass burning emissions, Environ. Chem., 13, 665–673, doi:10.1071/EN15174, 2016.

15 Chung, M. Y., Lazaro, R. A., Lim, D., Jackson, J., Lyon, J., Rendulic, D. and Hasson, A. S.: Aerosol-borne quinones and reactive oxygen species generation by particulate matter extracts, Environ. Sci. Technol., 40, 4880–4886, doi:10.1021/es0515957, 2006.

Dimashki, M.: Measurements of nitro-PAH in the atmospheres of two cities, Atmos. Environ., 34, 2459–2469, doi:10.1016/S1352-2310(99)00417-3, 2000.

20 Ding, J., Zhong, J., Yang, Y., Li, B., Shen, G., Su, Y., Wang, C., Li, W., Shen, H., Wang, B., Wang, R., Huang, Y., Zhang, Y., Cao, H., Zhu, Y., Simonich, S. L. M. and Tao, S.: Occurrence and exposure to polycyclic aromatic hydrocarbons and their derivatives in a rural Chinese home through biomass fuelled cooking, Environ. Pollut., 169, 160–166, doi:10.1016/j.envpol.2011.10.008, 2012.

Draxler, R. R. and Rolph, G. D.: HYSPLIT (hybrid single-particle lagrangian integrated trajectory) model access via
25 NOAA ARL READY, NOAA Air Resour. Lab. Silver Springs, USA. Available from: http://www.arl.noaa.gov/ready/hysplit4.html, 2003.

Endo, S. and Goss, K. U.: Applications of polyparameter linear free energy relationships in environmental chemistry, Environ. Sci. Technol., 48, 12477–12491, doi:10.1021/es503369t, 2014.

Enya, T., Suzuki, H., Watanabe, T., Hirayama, T. and Hisamatsu, Y.: 3-Nitrobenzanthrone, a powerful bacterial
30 mutagen and suspected human carcinogen found in diesel exhaust and airborne particulates, Environ. Sci. Technol., 31, 2772–2776, doi:10.1021/es961067i, 1997.

Finlayson-Pitts, B. and Pitts, J. N.: Chemistry of the upper and lower atmosphere: theory, experiments, application, Academic Press, San Diego, USA., 2000.

Ganranoo, L., Mishra, S. K., Azad, A. K., Shigihara, A., Dasgupta, P. K., Breitbach, Z. S., Armstrong, D. W., Grudpan,
35 K. and Rappenglueck, B.: Measurement of nitrophenols in rain and air by two-dimensional liquid chromatography-chemically active liquid core waveguide spectrometry, Anal. Chem., 82, 5838–5843, doi:10.1021/ac101015y, 2010.

Goss, K.-U., Buschmann, J. and Schwarzenbach, R. P.: Determination of the surface sorption properties of talc, different salts, and clay minerals at various relative humidities using adsorption data of a diverse set of organic vapors, Environ. Toxicol. Chem., 22, 2667–2672, doi:10.1897/03-56, 2003.

40 Harrison, M. A. J., Barra, S., Borghesi, D., Vione, D., Arsene, C. and Iulian Olariu, R.: Nitrated phenols in the atmosphere: a review, Atmos. Environ., 39, 231–248, doi:10.1016/j.atmosenv.2004.09.044, 2005.

Herterich, R. and Herrmann, R.: Comparing the distribution of nitrated phenols in the atmosphere of two German hill sites, Environ. Technol., 11, 961–972, doi:10.1080/09593339009384948, 1990.

Hinrichs, R. Z., Buczek, P. and Trivedi, J. J.: Solar absorption by aerosol-bound nitrophenols compared to aqueous
45 and gaseous nitrophenols, Environ. Sci. Technol., 50, 5661–5667, doi:10.1021/acs.est.6b00302, 2016.

Atmospheric
Chemistry
and Physics
Discussions

Open Access

Hoff, J. T., Wania, F., Mackay, D. and Gillham, R.: Sorption of nonpolar organic vapors by ice and snow, Environ. Sci. Technol., 29, 1982–1989, doi:10.1021/es00008a016, 1995.

Huang, Q., Wang, L. and Han, S.: The genotoxicity of substituted nitrobenzenes and the quantitative structure-activity relationship studies, Chemosphere, 30, 915–923, doi:10.1016/0045-6535(94)00450-9, 1995.

5 Huang, W., Huang, B., Bi, X., Lin, Q., Liu, M., Ren, Z., Zhang, G., Wang, X., Sheng, G. and Fu, J.: Emission of PAHs, NPAHs and OPAHs from residential honeycomb coal briquette combustion, Energy & Fuels, 28, 636–642, doi:10.1021/ef401901d, 2014.

Iinuma, Y., Brüggemann, E., Gnauk, T., Müller, K., Andreae, M. O., Helas, G., Parmar, R. and Herrmann, H.: Source characterization of biomass burning particles: The combustion of selected European conifers, African hardwood, 10 savanna grass, and German and Indonesian peat, J. Geophys. Res., 112, D08209, doi:10.1029/2006JD007120, 2007.

Iinuma, Y., Böge, O., Gräfe, R. and Herrmann, H.: Methyl-nitrocatechols: atmospheric tracer compounds for biomass burning secondary organic aerosols, Environ. Sci. Technol., 44, 8453–8459, doi:10.1021/es102938a, 2010.

Jaber, F., Schummer, C., Al Chami, J., Mirabel, P. and Millet, M.: Solid-phase microextraction and gas chromatography–mass spectrometry for analysis of phenols and nitrophenols in rainwater, as their t-butyldimethylsilyl 15 derivatives, Anal. Bioanal. Chem., 387, 2527–2535, doi:10.1007/s00216-006-1115-9, 2007.

Jariyasopit, N., Zimmermann, K., Schrlau, J., Arey, J., Atkinson, R., Yu, T.-W., Dashwood, R. H., Tao, S. and Simonich, S. L. M.: Heterogeneous reactions of particulate matter-bound PAHs and NPAHs with NO3/N2O5, OH radicals, and O3 under simulated long-range atmospheric transport conditions: reactivity and mutagenicity, Environ. Sci. Technol., 48, 10155–10164, doi:10.1021/es5015407, 2014.

20 Jonker, M. T. O. and Koelmans, A. A.: Sorption of polycyclic aromatic hydrocarbons and polychlorinated biphenyls to soot and soot-like materials in the aqueous environment: mechanistic considerations, Environ. Sci. Technol., 36, 3725–3734, doi:10.1021/es020019x, 2002.

Kahnt, A., Behrouzi, S., Vermeylen, R., Safi Shalamzari, M., Vercauteren, J., Roekens, E., Claeys, M. and Maenhaut, W.: One-year study of nitro-organic compounds and their relation to wood burning in PM10 aerosol from a rural site 25 in Belgium, Atmos. Environ., 81, 561–568, doi:10.1016/j.atmosenv.2013.09.041, 2013.

Kamprad, I. and Goss, K.-U.: Systematic investigation of the sorption properties of polyurethane foams for organic vapors, Anal. Chem., 79, 4222–4227, doi:10.1021/ac070265x, 2007.

Karavalakis, G., Deves, G., Fontaras, G., Stournas, S., Samaras, Z. and Bakeas, E.: The impact of soy-based biodiesel on PAH, nitro-PAH and oxy-PAH emissions from a passenger car operated over regulated and nonregulated driving 30 cycles, Fuel, 89, 3876–3883, doi:10.1016/j.fuel.2010.07.002, 2010.

Kawamura, K. and Kaplan, I. R.: Organic compounds in the rainwater of Los Angeles, Environ. Sci. Technol., 17, 497–501, doi:10.1021/es00114a011, 1983.

Kelly, F. J. and Fussell, J. C.: Role of oxidative stress in cardiovascular disease outcomes following exposure to ambient air pollution, Free Radic. Biol. Med., 110, 345–367, doi:10.1016/j.freeradbiomed.2017.06.019, 2017.

35 Keyte, I. J., Harrison, R. M. and Lammel, G.: Chemical reactivity and long-range transport potential of polycyclic aromatic hydrocarbons - a review, Chem. Soc. Rev., 42, 9333–9391, doi:10.1039/C3CS60147A, 2013.

Kitanovski, Z., Grgić, I., Vermeylen, R., Claeys, M. and Maenhaut, W.: Liquid chromatography tandem mass spectrometry method for characterization of monoaromatic nitro-compounds in atmospheric particulate matter, J. Chromatogr. A, 1268, 35–43, doi:10.1016/j.chroma.2012.10.021, 2012.

40 Kitanovski, Z., Čusak, A., Grgić, I. and Claeys, M.: Chemical characterization of the main products formed through aqueous-phase photonitration of guaiacol, Atmos. Meas. Tech., 7, 2457–2470, doi:10.5194/amt-7-2457-2014, 2014.

Kohler, M. and Heeb, N. V: Determination of nitrated phenolic compounds in rain by liquid chromatography/atmospheric pressure chemical ionization mass spectrometry, Anal. Chem., 75, 3115–3121, doi:10.1021/ac0264067, 2003.

Kojima, Y., Inazu, K., Hisamatsu, Y., Okochi, H., Baba, T. and Nagoya, T.: Influence of secondary formation on atmospheric occurrences of oxygenated polycyclic aromatic hydrocarbons in airborne particles, Atmos. Environ., 44, 2873–2880, doi:10.1016/j.atmosenv.2010.04.048, 2010.

Kovacic, P. and Somanathan, R.: Nitroaromatic compounds: environmental toxicity, carcinogenicity, mutagenicity, therapy and mechanism, J. Appl. Toxicol., 34, 810–824, doi:10.1002/jat.2980, 2014.

Kroflič, A., Grilc, M. and Grgić, I.: Does toxicity of aromatic pollutants increase under remote atmospheric conditions?, Sci. Rep., 5, 8859, doi:10.1038/srep08859, 2015.

Lammel, G.: Polycyclic aromatic compounds in the atmosphere – a review identifying research needs, Polycycl. Aromat. Compd., 35, 316–329, doi:10.1080/10406638.2014.931870, 2015.

Leuenberger, C., Ligocki, M. P. and Pankow, J. F.: Trace organic compounds in rain. 4. Identities, concentrations, and scavenging mechanisms for phenols in urban air and rain, Environ. Sci. Technol., 19, 1053–1058, doi:10.1021/es00141a005, 1985.

Leuenberger, C., Czuczwa, J., Tremp, J. and Giger, W.: Nitrated phenols in rain: atmospheric occurrence of phytotoxic pollutants, Chemosphere, 17, 511–515, doi:10.1016/0045-6535(88)90026-4, 1988.

Levsen, K., Behnert, S., Prieß, B., Svoboda, M., Winkeler, H.-D. and Zietlow, J.: Organic compounds in precipitation, Chemosphere, 21, 1037–1061, doi:10.1016/0045-6535(90)90127-F, 1990.

Levsen, K., Behnert, S. and Winkeler, H. D.: Organic compounds in precipitation, Fresenius. J. Anal. Chem., 340, 665–671, doi:10.1007/BF00321532, 1991.

Levsen, K., Behnert, S., Mußmann, P., Raabe, M. and Prieß, B.: Organic compounds in cloud and rain water, Int. J. Environ. Anal. Chem., 52, 87–97, doi:10.1080/03067319308042851, 1993.

Li, X., Jiang, L., Hoa, L. P., Lyu, Y., Xu, T., Yang, X., Iinuma, Y., Chen, J. and Herrmann, H.: Size distribution of particle-phase sugar and nitrophenol tracers during severe urban haze episodes in Shanghai, Atmos. Environ., 145, 115–127, doi:10.1016/j.atmosenv.2016.09.030, 2016.

Lide, D. R.: CRC Handbook of Chemistry and Physics, 90th ed., CRC Press, Boca Raton, USA, 2010.

Limbeck, A. and Puxbaum, H.: Dependence of in-cloud scavenging of polar organic aerosol compounds on the water solubility, J. Geophys. Res., 105, 19857–19867, doi:10.1029/2000JD900123, 2000.

Lin, P., Aiona, P. K., Li, Y., Shiraiwa, M., Laskin, J., Nizkorodov, S. A. and Laskin, A.: Molecular characterization of brown carbon in biomass burning aerosol particles, Environ. Sci. Technol., 50, 11815–11824, doi:10.1021/acs.est.6b03024, 2016.

Lin, Y., Ma, Y., Qiu, X., Li, R., Fang, Y., Wang, J., Zhu, Y. and Hu, D.: Sources, transformation, and health implications of PAHs and their nitrated, hydroxylated, and oxygenated derivatives in PM2.5 in Beijing, J. Geophys. Res., 120, 7219–7228, doi:10.1002/2015JD023628, 2015.

Lodovici, M. and Bigagli, E.: Oxidative Stress and Air Pollution Exposure, J. Toxicol., 2011, 1–9, doi:10.1155/2011/487074, 2011.

Mohr, C., Lopez-Hilfiker, F. D., Zotter, P., Prévoît, A. S. H., Xu, L., Ng, N. L., Herndon, S. C., Williams, L. R., Franklin, J. P., Zahniser, M. S., Worsnop, D. R., Knighton, W. B., Aiken, A. C., Gorkowski, K. J., Dubey, M. K., Allan, J. D. and Thornton, J. A.: Contribution of nitrated phenols to wood burning brown carbon light absorption in Detling, United Kingdom during winter time, Environ. Sci. Technol., 47, 6316–6324, doi:10.1021/es400683v, 2013.

Møller, P., Danielsen, P. H., Karottki, D. G., Jantzen, K., Roursgaard, M., Klingberg, H., Jensen, D. M., Christophersen, D. V., Hemmingsen, J. G., Cao, Y. and Loft, S.: Oxidative stress and inflammation generated DNA damage by exposure to air pollution particles, Mutat. Res. Rev. Mutat. Res., 762, 133–166, doi:10.1016/j.mrrev.2014.09.001, 2014.

Pflieger, M. and Kroflič, A.: Acute toxicity of emerging atmospheric pollutants from wood lignin due to biomass burning, J. Hazard. Mater., 338, 132–139, doi:10.1016/j.jhazmat.2017.05.023, 2017.

Pham, C. T., Kameda, T., Toriba, A. and Hayakawa, K.: Polycyclic aromatic hydrocarbons and nitropolycyclic aromatic hydrocarbons in particulates emitted by motorcycles, Environ. Pollut., 183, 175–183, doi:10.1016/j.envpol.2013.01.003, 2013.

5   Phousongphouang, P. T. and Arey, J.: Sources of the atmospheric contaminants, 2-nitrobenzanthrone and 3-nitrobenzanthrone, Atmos. Environ., 37, 3189–3199, doi:10.1016/S1352-2310(03)00344-3, 2003.

Rippen, G., Zietz, E., Frank, R., Knacker, T. and Klöpffer, W.: Do airborne nitrophenols contribute to forest decline?, Environ. Technol. Lett., 8, 475–482, doi:10.1080/09593338709384508, 1987.

Rogge, W. F., Mazurek, M. A., Hildemann, L. M., Cass, G. R. and Simoneit, B. R. T.: Quantification of urban organic aerosols at a molecular level: identification, abundance and seasonal variation, Atmos. Environ., 27, 1309–1330,
10   doi:10.1016/0960-1686(93)90257-Y, 1993.

Roth, C. M., Goss, K.-U. and Schwarzenbach, R. P.: Sorption of a diverse set of organic vapors to diesel soot and road tunnel aerosols, Environ. Sci. Technol., 39, 6632–6637, doi:10.1021/es049204w, 2005.

Schummer, C., Groff, C., Al Chami, J., Jaber, F. and Millet, M.: Analysis of phenols and nitrophenols in rainwater collected simultaneously on an urban and rural site in east of France, Sci. Total Environ., 407, 5637–5643,
15   doi:10.1016/j.scitotenv.2009.06.051, 2009.

Schüssler, W. and Nitschke, L.: Nitrophenols in precipitation, Chemosphere, 42, 277–283, doi:10.1016/S0045-6535(00)00086-2, 2001.

Shahpoury, P., Lammel, G., Holubová Šmejkalová, A., Klánová, J., Přibylová, P. and Váňa, M.: Polycyclic aromatic hydrocarbons, polychlorinated biphenyls, and chlorinated pesticides in background air in central Europe –
20   investigating parameters affecting wet scavenging of polycyclic aromatic hydrocarbons, Atmos. Chem. Phys., 15, 1795–1805, doi:10.5194/acp-15-1795-2015, 2015.

Shahpoury, P., Lammel, G., Albinet, A., Sofuoğlu, A., Dumanoğlu, Y., Sofuoğlu, S. C., Wagner, Z. and Zdimal, V.: Evaluation of a conceptual model for gas-particle partitioning of polycyclic aromatic hydrocarbons using polyparameter linear free energy relationships, Environ. Sci. Technol., 50, 12312–12319,
25   doi:10.1021/acs.est.6b02158, 2016.

Sharma, M. and McBean, E. A.: Atmospheric PAH deposition: deposition velocities and washout ratios, J. Environ. Eng., 128, 186–195, doi:10.1061/(ASCE)0733-9372(2002)128:2(186), 2002.

Shen, G., Tao, S., Wei, S., Zhang, Y., Wang, R., Wang, B., Li, W., Shen, H., Huang, Y., Chen, Y., Chen, H., Yang, Y., Wang, W., Wang, X., Liu, W. and Simonich, S. L. M.: Emissions of parent, nitro, and oxygenated polycyclic
30   aromatic hydrocarbons from residential wood combustion in rural China, Environ. Sci. Technol., 46, 8123–8130, doi:10.1021/es301146v, 2012.

Shen, G., Xue, M., Wei, S., Chen, Y., Wang, B., Wang, R., Lv, Y., Shen, H., Li, W., Zhang, Y., Huang, Y., Chen, H., Wei, W., Zhao, Q., Li, B., Wu, H. and Tao, S.: Emissions of parent, nitrated, and oxygenated polycyclic aromatic hydrocarbons from indoor corn straw burning in normal and controlled combustion conditions, J. Environ. Sci., 25,
35   2072–2080, doi:10.1016/S1001-0742(12)60249-6, 2013a.

Shen, G., Tao, S., Wei, S., Chen, Y., Zhang, Y., Shen, H., Huang, Y., Zhu, D., Yuan, C., Wang, H., Wang, Y., Pei, L., Liao, Y., Duan, Y., Wang, B., Wang, R., Lv, Y., Li, W., Wang, X. and Zheng, X.: Field measurement of emission factors of PM, EC, OC, parent, nitro-, and oxy- polycyclic aromatic hydrocarbons for residential briquette, coal cake, and wood in rural Shanxi, China, Environ. Sci. Technol., 47, 2998–3005, doi:10.1021/es304599g, 2013b.

40   Souza, K. F., Carvalho, L. R. F., Allen, A. G. and Cardoso, A. A.: Diurnal and nocturnal measurements of PAH, nitro-PAH, and oxy-PAH compounds in atmospheric particulate matter of a sugar cane burning region, Atmos. Environ., 83, 193–201, doi:10.1016/j.atmosenv.2013.11.007, 2014.

Teich, M., Van Pinxteren, D., Wang, M., Kecorius, S., Wang, Z., Müller, T., Močnik, G. and Herrmann, H.: Contributions of nitrated aromatic compounds to the light absorption of water-soluble and particulate brown carbon
45   in different atmospheric environments in Germany and China, Atmos. Chem. Phys., 17, 1653–1672, doi:10.5194/acp-17-1653-2017, 2017.

Tomaz, S., Shahpoury, P., Jaffrezo, J.-L., Lammel, G., Perraudin, E., Villenave, E. and Albinet, A.: One-year study of polycyclic aromatic compounds at an urban site in Grenoble (France): seasonal variations, gas/particle partitioning and cancer risk estimation, Sci. Total Environ., 565, 1071–1083, doi:10.1016/j.scitotenv.2016.05.137, 2016.

5 Vanni, A., Pellegrino, V., Gamberini, R. and Calabria, A.: An Evidence for nitrophenols contamination in Antarctic fresh-water and snow. Simultaneous determination of nitrophenols and nitroarenes at ng/L levels, Int. J. Environ. Anal. Chem., 79, 349–365, doi:10.1080/03067310108044394, 2001.

Vicente, E. D., Vicente, A. M., Musa Bandowe, B. A. and Alves, C. A.: Particulate phase emission of parent polycyclic aromatic hydrocarbons (PAHs) and their derivatives (alkyl-PAHs, oxygenated-PAHs, azaarenes and nitrated PAHs) from manually and automatically fired combustion appliances, Air Qual. Atmos. Heal., 9, 653–668,
10 doi:10.1007/s11869-015-0364-1, 2016.

Walgraeve, C., Demeestere, K., Dewulf, J., Zimmermann, R. and Van Langenhove, H.: Oxygenated polycyclic aromatic hydrocarbons in atmospheric particulate matter: molecular characterization and occurrence, Atmos. Environ., 44, 1831–1846, doi:10.1016/j.atmosenv.2009.12.004, 2010.

Watanabe, M. and Noma, Y.: Influence of combustion temperature on formation of nitro-PAHs and decomposition
15 and removal behaviors in pilot-scale waste incinerator, Environ. Sci. Technol., 43, 2512–2518, doi:10.1021/es8035169, 2009.

WHO: World Health Organization, environmental health criteria 220, dinitro-ortho-cresol, Geneva, Schwitzerland. Available from: www.who.int/ipcs/publications/ehc/en/ehc220.pdf, 2000.

Yang, B., Zhang, H., Wang, Y., Zhang, P., Shu, J., Sun, W. and Ma, P.: Experimental and theoretical studies on gas-
20 phase reactions of NO3 radicals with three methoxyphenols: guaiacol, creosol, and syringol, Atmos. Environ., 125, 243–251, doi:10.1016/j.atmosenv.2015.11.028, 2016.

Zhang, L., Wang, X., Moran, M. D. and Feng, J.: Review and uncertainty assessment of size-resolved scavenging coefficient formulations for below-cloud snow scavenging of atmospheric aerosols, Atmos. Chem. Phys., 13, 10005–10025, doi:10.5194/acp-13-10005-2013, 2013.

25 Zhuo, S., Du, W., Shen, G., Li, B., Liu, J., Cheng, H., Xing, B. and Tao, S.: Estimating relative contributions of primary and secondary sources of ambient nitrated and oxygenated polycyclic aromatic hydrocarbons, Atmos. Environ., 159, 126–134, doi:10.1016/j.atmosenv.2017.04.003, 2017.

Zielinska, B., Sagebiel, J., McDonald, J. D., Whitney, K. and Lawson, D. R.: Emission rates and comparative chemical composition from selected in-use diesel and gasoline-fueled vehicles, J. Air Waste Manage. Assoc., 54, 1138–1150,
30 doi:10.1080/10473289.2004.10470973, 2004.

Atmospheric
Chemistry
and Physics
Open Access
EGU
Discussions

Table 1. Sampling site details

|	Coordinates	Sampling date	Snowfall started	Sample collected
Urban				
Ub1 Mainz	49.99° N, 8.23° E	23 Feb 2015	8:00	12:45
Ub2 Götzens	47.23° N, 11.31° E	25 Feb 2015	Overnight	9:00
Ub3 Ostrava	49.86° N, 18.26° E	19 Feb 2016	14:00	19:00
Ub4 Mainz	49.99° N, 8.23° E	10 Jan 2017	9:00	15:00
Rural				
Rr1 Winterberg	51.18° N, 8.49° E	03 Mar 2015	15:00	18:30
Rr2 Altenberg	50.78° N, 13.69° E	05 Mar 2015	Overnight	8:00
Rr3 Kolsassberg	47.28° N, 11.65° E	25 Feb 2015	Overnight	10:00
Rr4 Pustá Polom 1	49.86° N, 17.98° E	19 Feb 2016	9:30	23:00
Rr5 Pustá Polom 2	49.86° N, 17.98° E	23 Feb 2016	14:00	23:00
Remote				
Rm1 Tempelfjorden	78.45° N 17.32° E	4 Mar 2015	1 Mar 2015	after snowfall [a]

[a] old snow, which had fallen 3-2 days before sampling

Atmospheric
Chemistry
and Physics
Discussions

Table 2. Target compound list

Analyte	Abbreviation	RT	Q1
1-Nitronaphthalene	1-NNAP	12.12	173.1
2-Nitronaphthalene	2-NNAP	12.62	173.1
5-Nitroacenaphthene	5-NACE	17.52	199.1
2-Nitrofluorene	2-NFLN	19.07	211.1
9-Nitroanthracene	9-NANT	19.46	223.1
9-Nitrophenanthrene	9-NPHE	20.64	223.1
3-Nitrophenanthrene	3-NPHE	21.4	223.1
2-Nitrofluoranthene	2-NFLT	25.75	247.1
3-Nitrofluoranthene	3-NFLT	25.80	247.1
1-Nitropyrene	1-NPYR	26.63	247.1
2-Nitropyrene	2-NPYR	26.95	247.1
7-Nitrobenz(a)anthracene	7-NBAA	29.41	273.1
6-Nitrochrysene	6-NCHR	30.66	273.1
1,3-Dinitropyrene	1,3-N2PYR	31.8	292.1
1,6-Dinitropyrene	1,6-N2PYR	32.81	292.1
1,8-Dinitropyrene	1,8-N2PYR	33.54	292.1
6-Nitrobenz(a)pyrene	6-NBAP	36.73	297.1
1,4-Naphthoquinone	1,4-O_2NAP	10.18	158.1
9-Fluorenone	9-OFLN	13.78	180.1
9,10-Anthraquinone	9,10-O_2ANT	17.03	208.1
Acenaphthoquinone	O_2ACE	17.82	198.1
2-Nitro-9-fluorenone	2-N-9-OFLN	20.54	225.1
Benz(a)fluorenone	BaOFLN	22.88	230.1
Benz(b)fluorenone	BbOFLN	23.82	230.1
Benzanthrone	OBAT	25.07	230.1
1,2-Benzanthraquinone	1,2-O_2BAA	26.46	258.1
3-Nitrosalicylic acid	3-NSA	3.60	182
5-Nitrosalicylic acid	5-NSA	5.07	182
4-Nitrocatechol	4-NC	7.76	154
4-nitroguaiacol	4-NG	8.29	168
4-Methyl-5-nitrocatechol	4-M-5-NC	9.47	168
4-Nitrophenol	4-NP	10.00	138
2,4-Dinitrophenol	2,4-DNP	10.92	183
3-Methyl-4-nitrophenol	3-M-4-NP	13.19	152
3-Methyl-5-nitrocatechol	3-M-5-NC	14.01	168
2-Methyl-4-nitrophenol	2-M-4-NP	16.72	152
Dinitro-ortho-cresol	DNOC	17.05	197

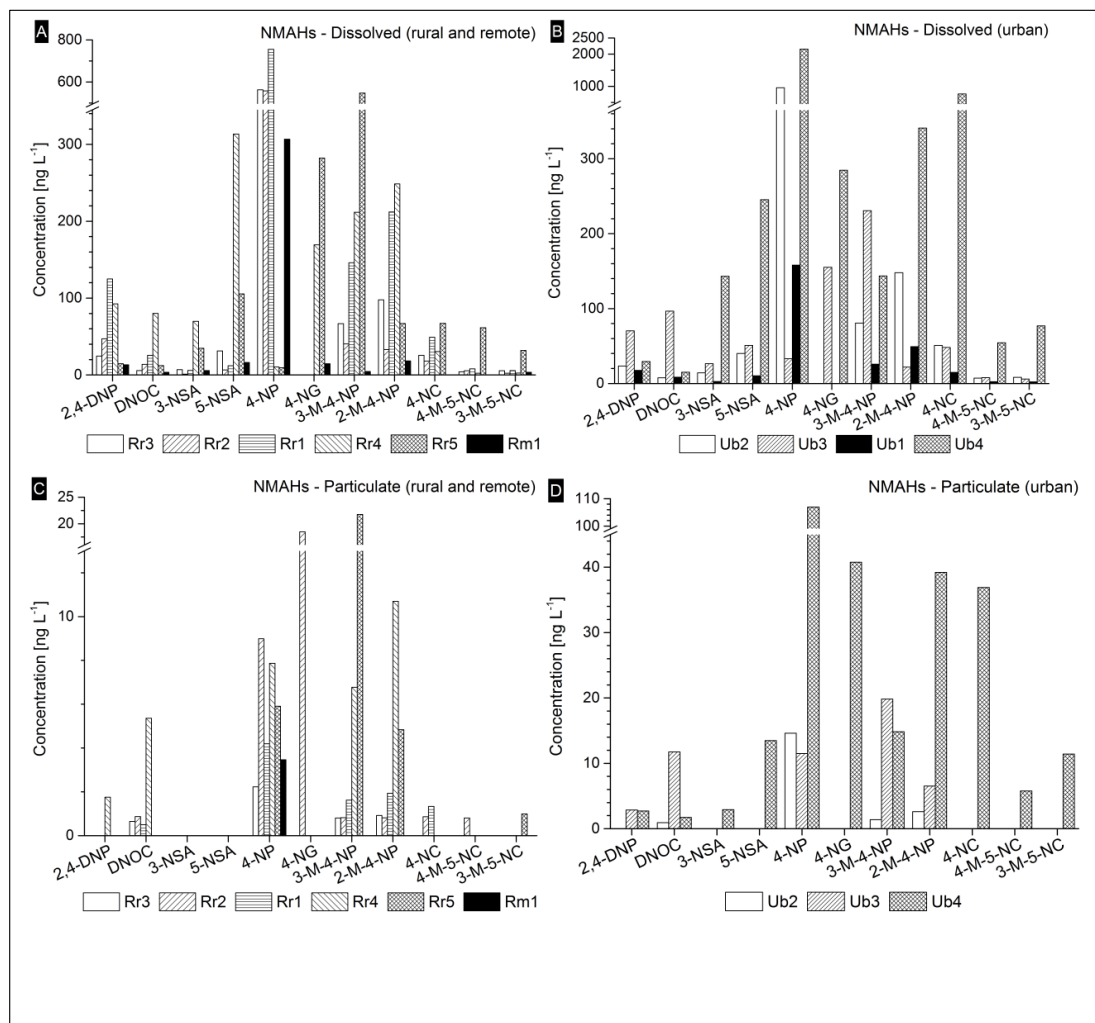Abbreviations, retention times (RT), and quantification ions (Q1) of target analytes

Atmospheric
Chemistry
and Physics
Discussions

Figure 1 N/OPAHs found in snow samples
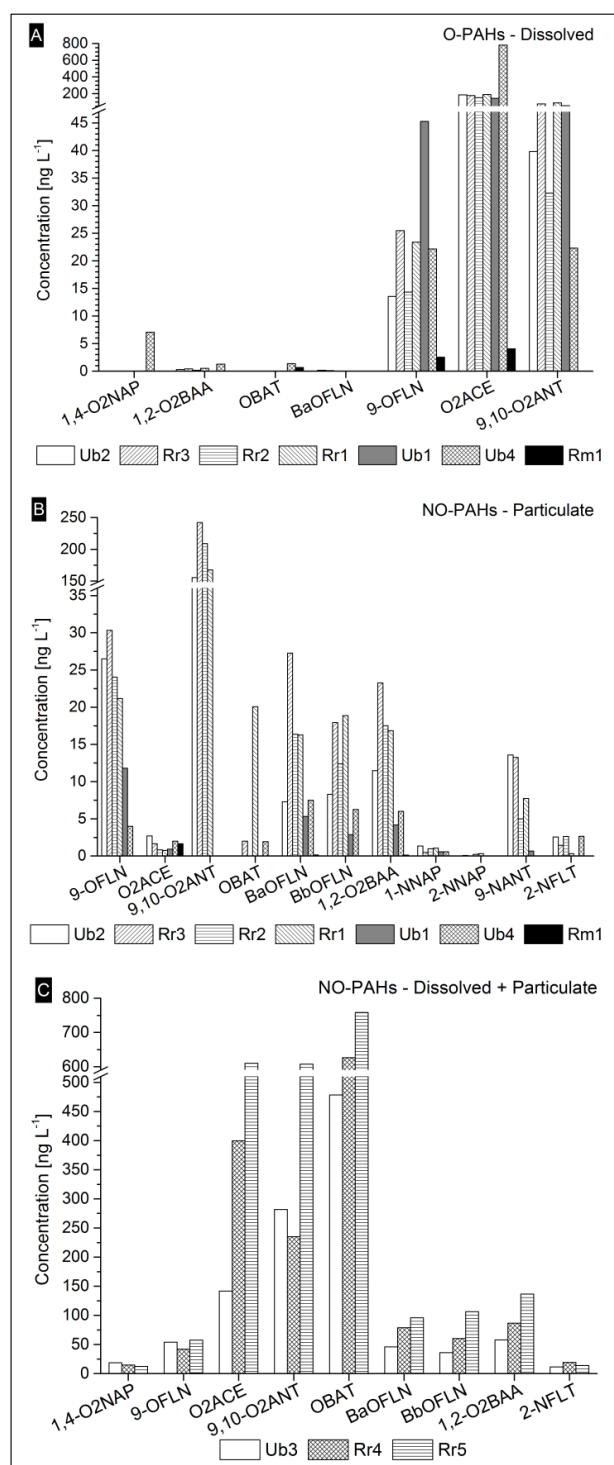
Figure 2 NMAHs found in snow samples

Atmospheric
Chemistry
and Physics

Open Access

Discussions
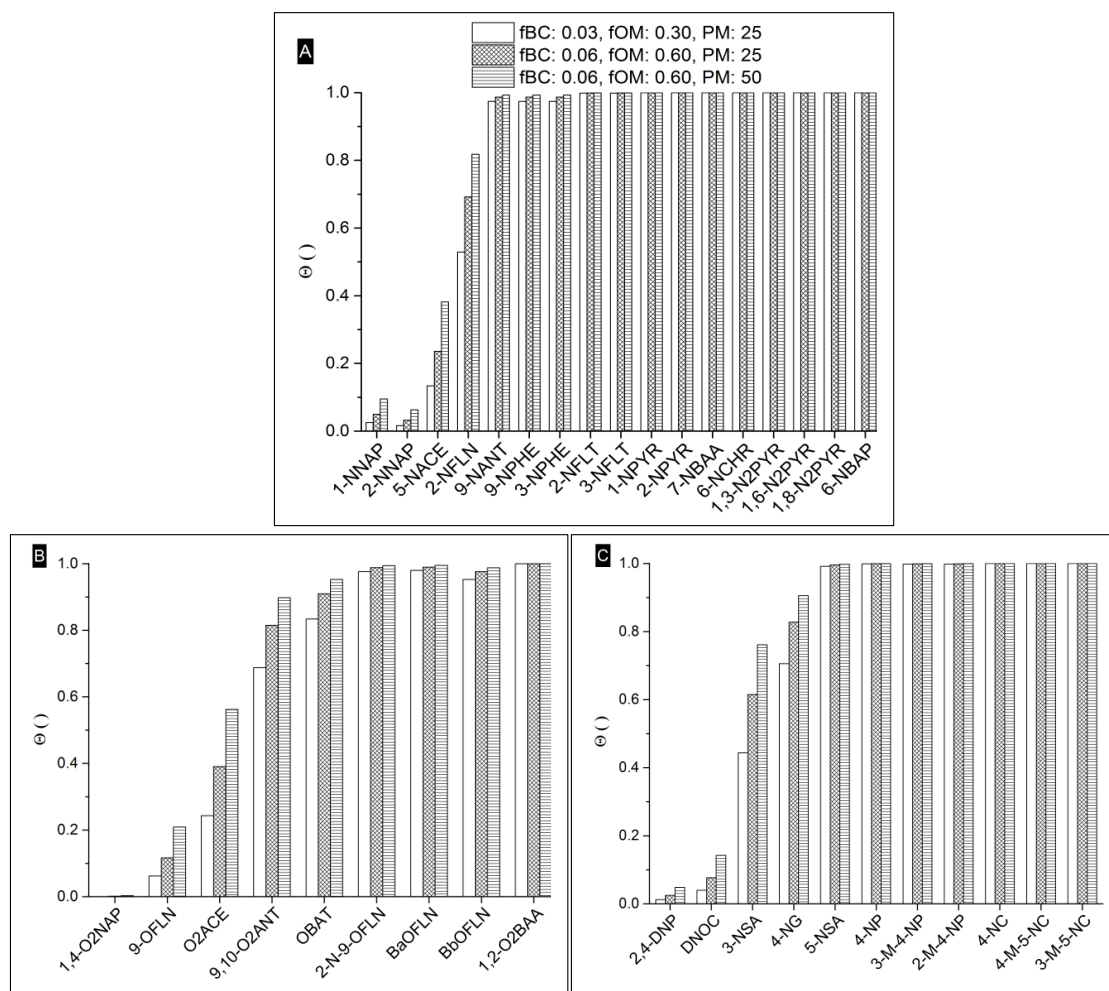
EGU

Figure 3 Particulate mass fractions Θ estimated at 273 K using multiphase gas-particle partitioning model for NPAHs (A), OPAHs (B), and NMAHs (C)

Figure 4 Fraction of N/OPAHs (A) and NMAHs (B) removed by particle scavenging (Θ_W)